A novel method for modeling the recoil in W boson events at hadron colliders

V.M. Abazov[ak], B. Abbott[bw], M. Abolins[bm], B.S. Acharya[ad], M. Adams[ay], T. Adams[aw], E. Aguilo[f],
M. Ahsan[bg], G.D. Alexeev[ak], G. Alkhazov[ao], A. Alton[bl,1], G. Alverson[bk], G.A. Alves[b], L.S. Ancu[aj],
T. Andeen[ba], M.S. Anzelc[ba], M. Aoki[ax], Y. Arnoud[n], M. Arov[bh], M. Arthaud[r], A. Askew[aw,2], B. Åsman[ap],
O. Atramentov[aw,2], C. Avila[h], J. BackusMayes[cd], F. Badaud[m], L. Bagby[ax], B. Baldin[ax], D.V. Bandurin[bg],
S. Banerjee[ad], E. Barberis[bk], A.-F. Barfuss[o], P. Bargassa[cb], P. Baringer[bf], J. Barreto[b], J.F. Bartlett[ax],
U. Bassler[r], D. Bauer[ar], S. Beale[f], A. Bean[bf], M. Begalli[c], M. Begel[bu], C. Belanger-Champagne[ap],
L. Bellantoni[ax], A. Bellavance[ax], J.A. Benitez[bm], S.B. Beri[ab], G. Bernardi[q], R. Bernhard[w], I. Bertram[aq],
M. Besançon[r], R. Beuselinck[ar], V.A. Bezzubov[an], P.C. Bhat[ax], V. Bhatnagar[ab], G. Blazey[az], S. Blessing[aw],
K. Bloom[bo], A. Boehnlein[ax], D. Boline[bj], T.A. Bolton[bg], E.E. Boos[am], G. Borissov[aq], T. Bose[bj],
A. Brandt[bz], R. Brock[bm], G. Brooijmans[br], A. Bross[ax], D. Brown[s], X.B. Bu[g], D. Buchholz[ba],
M. Buehler[cc], V. Buescher[v], V. Bunichev[am], S. Burdin[aq,3], T.H. Burnett[cd], C.P. Buszello[ar], P. Calfayan[z],
B. Calpas[o], S. Calvet[p], J. Cammin[bs], M.A. Carrasco-Lizarraga[ah], E. Carrera[aw], W. Carvalho[c],
B.C.K. Casey[ax], H. Castilla-Valdez[ah], S. Chakrabarti[bt], D. Chakraborty[az], K.M. Chan[bc], A. Chandra[av],
E. Cheu[at], D.K. Cho[bj], S.W. Cho[af], S. Choi[ag], B. Choudhary[ac], T. Christoudias[ar], S. Cihangir[ax],
D. Claes[bo], J. Clutter[bf], M. Cooke[ax], W.E. Cooper[ax], M. Corcoran[cb], F. Couderc[r], M.-C. Cousinou[o],
D. Cutts[by], M. Ćwiok[ae], A. Das[at], G. Davies[ar], K. De[bz], S.J. de Jong[aj], E. De La Cruz-Burelo[ah],
K. DeVaughan[bo], F. Déliot[r], M. Demarteau[ax], R. Demina[bs], D. Denisov[ax], S.P. Denisov[an], S. Desai[ax],
H.T. Diehl[ax], M. Diesburg[ax], A. Dominguez[bo], T. Dorland[cd], A. Dubey[ac], L.V. Dudko[am], L. Duflot[p],
D. Duggan[aw], A. Duperrin[o], S. Dutt[ab], A. Dyshkant[az], M. Eads[bo], D. Edmunds[bm], J. Ellison[av],
V.D. Elvira[ax], Y. Enari[by], S. Eno[bi], M. Escalier[o], H. Evans[bb], A. Evdokimov[bu], V.N. Evdokimov[an],
G. Facini[bk], A.V. Ferapontov[bg], T. Ferbel[bi,bs], F. Fiedler[y], F. Filthaut[aj], W. Fisher[ax], H.E. Fisk[ax],
M. Fortner[az], H. Fox[aq], S. Fu[ax], S. Fuess[ax], T. Gadfort[br], C.F. Galea[aj], A. Garcia-Bellido[bs], V. Gavrilov[al],
P. Gay[m], W. Geist[s], W. Geng[o,bm], C.E. Gerber[ay], Y. Gershtein[aw,2], D. Gillberg[f], G. Ginther[ax,bs],
B. Gómez[h], A. Goussiou[cd], P.D. Grannis[bt], S. Greder[s], H. Greenlee[ax], Z.D. Greenwood[bh], E.M. Gregores[d],
G. Grenier[t], Ph. Gris[m], J.-F. Grivaz[p], A. Grohsjean[r], S. Grünendahl[ax], M.W. Grünewald[ae], F. Guo[bt],
J. Guo[bt], G. Gutierrez[ax], P. Gutierrez[bw], A. Haas[br], P. Haefner[z], S. Hagopian[aw], J. Haley[bp], I. Hall[bm],
R.E. Hall[au], L. Han[g], K. Harder[as], A. Harel[bs], J.M. Hauptman[be], J. Hays[ar], T. Hebbeker[u], D. Hedin[az],
J.G. Hegeman[ai], A.P. Heinson[av], U. Heintz[bj], C. Hensel[x], I. Heredia-De La Cruz[ah], K. Herner[bl],
G. Hesketh[bk], M.D. Hildreth[bc], R. Hirosky[cc], T. Hoang[aw], J.D. Hobbs[bt], B. Hoeneisen[l], M. Hohlfeld[v],
S. Hossain[bw], P. Houben[ai], Y. Hu[bt], Z. Hubacek[j], N. Huske[q], V. Hynek[j], I. Iashvili[bq], R. Illingworth[ax],
A.S. Ito[ax], S. Jabeen[bj], M. Jaffré[p], S. Jain[bw], K. Jakobs[w], D. Jamin[o], R. Jesik[ar], K. Johns[at],
C. Johnson[br], M. Johnson[ax], D. Johnston[bo], A. Jonckheere[ax], P. Jonsson[ar], A. Juste[ax], E. Kajfasz[o],
D. Karmanov[am], P.A. Kasper[ax], I. Katsanos[bo], V. Kaushik[bz], R. Kehoe[ca], S. Kermiche[o], N. Khalatyan[ax],
A. Khanov[bx], A. Kharchilava[bq], Y.N. Kharzheev[ak], D. Khatidze[by], M.H. Kirby[ba], M. Kirsch[u], B. Klima[ax],
J.M. Kohli[ab], J.-P. Konrath[w], A.V. Kozelov[an], J. Kraus[bm], T. Kuhl[y], A. Kumar[bq], A. Kupco[k], T. Kurča[t],
V.A. Kuzmin[am], J. Kvita[i], F. Lacroix[m], D. Lam[bc], S. Lammers[bb], G. Landsberg[by], P. Lebrun[t], H.S. Lee[af],
W.M. Lee[ax], A. Leflat[am], J. Lellouch[q], L. Li[av], Q.Z. Li[ax], S.M. Lietti[e], J.K. Lim[af], D. Lincoln[ax],
J. Linnemann[bm], V.V. Lipaev[an], R. Lipton[ax], Y. Liu[g], Z. Liu[f], A. Lobodenko[ao], M. Lokajicek[k], P. Love[aq],
H.J. Lubatti[cd], R. Luna-Garcia[ah,4], A.L. Lyon[ax], A.K.A. Maciel[b], D. Mackin[cb], P. Mättig[aa],
R. Magaña-Villalba[ah], P.K. Mal[at], S. Malik[bo], V.L. Malyshev[ak], Y. Maravin[bg], B. Martin[n],
R. McCarthy[bt], C.L. McGivern[bf], M.M. Meijer[aj], A. Melnitchouk[bn], L. Mendoza[h], D. Menezes[az],
P.G. Mercadante[e], M. Merkin[am], K.W. Merritt[ax], A. Meyer[u], J. Meyer[x], N.K. Mondal[ad],
H.E. Montgomery[ax], R.W. Moore[f], T. Moulik[bf], G.S. Muanza[o], M. Mulhearn[br], O. Mundal[v], L. Mundim[c],
E. Nagy[o], M. Naimuddin[ax], M. Narain[by], H.A. Neal[bl], J.P. Negret[h], P. Neustroev[ao], H. Nilsen[w],
H. Nogima[c], S.F. Novaes[e], T. Nunnemann[z], G. Obrant[ao], C. Ochando[p], D. Onoprienko[bg], J. Orduna[ah],
N. Oshima[ax], N. Osman[ar], J. Osta[bc], R. Otec[j], G.J. Otero y Garzón[a], M. Owen[as], M. Padilla[av],

P. Padley[cb], M. Pangilinan[by], N. Parashar[bd], S.-J. Park[x], S.K. Park[af], J. Parsons[br], R. Partridge[by], N. Parua[bb], A. Patwa[bu], B. Penning[w], M. Perfilov[am], K. Peters[as], Y. Peters[as], P. Pétroff[p], R. Piegaia[a], J. Piper[bm], M.-A. Pleier[v], P.L.M. Podesta-Lerma[ah,1], V.M. Podstavkov[ax], Y. Pogorelov[bc], M.-E. Pol[b], P. Polozov[al], A.V. Popov[an], M. Prewitt[cb], S. Protopopescu[bu], J. Qian[bl], A. Quadt[x], B. Quinn[bn], A. Rakitine[aq], M.S. Rangel[p], K. Ranjan[ac], P.N. Ratoff[aq], P. Renkel[ca], P. Rich[as], M. Rijssenbeek[bt], I. Ripp-Baudot[s], F. Rizatdinova[bx], S. Robinson[ar], M. Rominsky[bw], C. Royon[r], P. Rubinov[ax], R. Ruchti[bc], G. Safronov[al], G. Sajot[n], A. Sánchez-Hernández[ah], M.P. Sanders[z], B. Sanghi[ax], G. Savage[ax], L. Sawyer[bh], T. Scanlon[ar], D. Schaile[z], R.D. Schamberger[bt], Y. Scheglov[ao], H. Schellman[ba], T. Schliephake[aa], S. Schlobohm[cd], C. Schwanenberger[as], R. Schwienhorst[bm], J. Sekaric[aw], H. Severini[bw], E. Shabalina[x], M. Shamim[bg], V. Shary[r], A.A. Shchukin[an], R.K. Shivpuri[ac], V. Siccardi[s], V. Simak[j], V. Sirotenko[ax], P. Skubic[bw], P. Slattery[bs], D. Smirnov[bc], G.R. Snow[bo], J. Snow[bv], S. Snyder[bu], S. Söldner-Rembold[as], L. Sonnenschein[u], A. Sopczak[aq], M. Sosebee[bz], K. Soustruznik[i], B. Spurlock[bz], J. Stark[n], V. Stolin[al], D.A. Stoyanova[an], J. Strandberg[bl], M.A. Strang[bq], E. Strauss[bt], M. Strauss[bw], R. Ströhmer[z], D. Strom[ay], L. Stutte[ax], S. Sumowidagdo[aw], P. Svoisky[aj], M. Takahashi[as], A. Tanasijczuk[a], W. Taylor[f], B. Tiller[z], M. Titov[r], V.V. Tokmenin[ak], I. Torchiani[w], D. Tsybychev[bt], B. Tuchming[r], C. Tully[bp], P.M. Tuts[br], R. Unalan[bm], L. Uvarov[ao], S. Uvarov[ao], S. Uzunyan[az], P.J. van den Berg[ai], R. Van Kooten[bb], W.M. van Leeuwen[ai], N. Varelas[ay], E.W. Varnes[at], I.A. Vasilyev[an], P. Verdier[t], L.S. Vertogradov[ak], M. Verzocchi[ax], M. Vesterinen[as], D. Vilanova[r], P. Vint[ar], P. Vokac[j], R. Wagner[bp], H.D. Wahl[aw], M.H.L.S. Wang[bs], J. Warchol[bc], G. Watts[cd], M. Wayne[bc], G. Weber[y], M. Weber[ax,6], L. Welty-Rieger[bb], A. Wenger[w,7], M. Wetstein[bi], A. White[bz], D. Wicke[y], M.R.J. Williams[aq], G.W. Wilson[bf], S.J. Wimpenny[av], M. Wobisch[bh], D.R. Wood[bk], T.R. Wyatt[as], Y. Xie[by], C. Xu[bl], S. Yacoob[ba], R. Yamada[ax], W.-C. Yang[as], T. Yasuda[ax], Y.A. Yatsunenko[ak], Z. Ye[ax], H. Ying[g], K. Yip[bu], H.D. Yoo[by], S.W. Youn[ax], J. Yu[bz], C. Zeitnitz[aa], S. Zelitch[cc], T. Zhao[cd], B. Zhou[bl], J. Zhu[bt], M. Zielinski[bs], D. Zieminska[bb], L. Zivkovic[br], V. Zutshi[az], E.G. Zverev[am]

(The DØ Collaboration)

[a] *Universidad de Buenos Aires, Buenos Aires, Argentina*
[b] *LAFEX, Centro Brasileiro de Pesquisas Físicas, Rio de Janeiro, Brazil*
[c] *Universidade do Estado do Rio de Janeiro, Rio de Janeiro, Brazil*
[d] *Universidade Federal do ABC, Santo André, Brazil*
[e] *Instituto de Física Teórica, Universidade Estadual Paulista, São Paulo, Brazil*
[f] *University of Alberta, Edmonton, Alberta, Canada; Simon Fraser University, Burnaby, British Columbia, Canada; York University, Toronto, Ontario, Canada and McGill University, Montreal, Quebec, Canada*
[g] *University of Science and Technology of China, Hefei, People's Republic of China*
[h] *Universidad de los Andes, Bogotá, Colombia*
[i] *Center for Particle Physics, Charles University, Faculty of Mathematics and Physics, Prague, Czech Republic*
[j] *Czech Technical University in Prague, Prague, Czech Republic*
[k] *Center for Particle Physics, Institute of Physics, Academy of Sciences of the Czech Republic, Prague, Czech Republic*
[l] *Universidad San Francisco de Quito, Quito, Ecuador*
[m] *LPC, Université Blaise Pascal, CNRS/IN2P3, Clermont, France*
[n] *LPSC, Université Joseph Fourier Grenoble 1, CNRS/IN2P3, Institut National Polytechnique de Grenoble, Grenoble, France*
[o] *CPPM, Aix-Marseille Université, CNRS/IN2P3, Marseille, France*
[p] *LAL, Université Paris-Sud, IN2P3/CNRS, Orsay, France*
[q] *LPNHE, IN2P3/CNRS, Universités Paris VI and VII, Paris, France*
[r] *CEA, Irfu, SPP, Saclay, France*
[s] *IPHC, Université de Strasbourg, CNRS/IN2P3, Strasbourg, France*
[t] *IPNL, Université Lyon 1, CNRS/IN2P3, Villeurbanne, France and Université de Lyon, Lyon, France*
[u] *III. Physikalisches Institut A, RWTH Aachen University, Aachen, Germany*
[v] *Physikalisches Institut, Universität Bonn, Bonn, Germany*
[w] *Physikalisches Institut, Universität Freiburg, Freiburg, Germany*
[x] *II. Physikalisches Institut, Georg-August-Universität Göttingen, Göttingen, Germany*
[y] *Institut für Physik, Universität Mainz, Mainz, Germany*
[z] *Ludwig-Maximilians-Universität München, München, Germany*
[aa] *Fachbereich Physik, University of Wuppertal, Wuppertal, Germany*
[ab] *Panjab University, Chandigarh, India*
[ac] *Delhi University, Delhi, India*
[ad] *Tata Institute of Fundamental Research, Mumbai, India*

2

[ae] University College Dublin, Dublin, Ireland

[af] Korea Detector Laboratory, Korea University, Seoul, Korea

[ag] SungKyunKwan University, Suwon, Korea

[ah] CINVESTAV, Mexico City, Mexico

[ai] FOM-Institute NIKHEF and University of Amsterdam/NIKHEF, Amsterdam, The Netherlands

[aj] Radboud University Nijmegen/NIKHEF, Nijmegen, The Netherlands

[ak] Joint Institute for Nuclear Research, Dubna, Russia

[al] Institute for Theoretical and Experimental Physics, Moscow, Russia

[am] Moscow State University, Moscow, Russia

[an] Institute for High Energy Physics, Protvino, Russia

[ao] Petersburg Nuclear Physics Institute, St. Petersburg, Russia

[ap] Stockholm University, Stockholm, Sweden, and Uppsala University, Uppsala, Sweden

[aq] Lancaster University, Lancaster, United Kingdom

[ar] Imperial College, London, United Kingdom

[as] University of Manchester, Manchester, United Kingdom

[at] University of Arizona, Tucson, Arizona 85721, USA

[au] California State University, Fresno, California 93740, USA

[av] University of California, Riverside, California 92521, USA

[aw] Florida State University, Tallahassee, Florida 32306, USA

[ax] Fermi National Accelerator Laboratory, Batavia, Illinois 60510, USA

[ay] University of Illinois at Chicago, Chicago, Illinois 60607, USA

[az] Northern Illinois University, DeKalb, Illinois 60115, USA

[ba] Northwestern University, Evanston, Illinois 60208, USA

[bb] Indiana University, Bloomington, Indiana 47405, USA

[bc] University of Notre Dame, Notre Dame, Indiana 46556, USA

[bd] Purdue University Calumet, Hammond, Indiana 46323, USA

[be] Iowa State University, Ames, Iowa 50011, USA

[bf] University of Kansas, Lawrence, Kansas 66045, USA

[bg] Kansas State University, Manhattan, Kansas 66506, USA

[bh] Louisiana Tech University, Ruston, Louisiana 71272, USA

[bi] University of Maryland, College Park, Maryland 20742, USA

[bj] Boston University, Boston, Massachusetts 02215, USA

[bk] Northeastern University, Boston, Massachusetts 02115, USA

[bl] University of Michigan, Ann Arbor, Michigan 48109, USA

[bm] Michigan State University, East Lansing, Michigan 48824, USA

[bn] University of Mississippi, University, Mississippi 38677, USA

[bo] University of Nebraska, Lincoln, Nebraska 68588, USA

[bp] Princeton University, Princeton, New Jersey 08544, USA

[bq] State University of New York, Buffalo, New York 14260, USA

[br] Columbia University, New York, New York 10027, USA

[bs] University of Rochester, Rochester, New York 14627, USA

[bt] State University of New York, Stony Brook, New York 11794, USA

[bu] Brookhaven National Laboratory, Upton, New York 11973, USA

[bv] Langston University, Langston, Oklahoma 73050, USA

[bw] University of Oklahoma, Norman, Oklahoma 73019, USA

[bx] Oklahoma State University, Stillwater, Oklahoma 74078, USA

[by] Brown University, Providence, Rhode Island 02912, USA

[bz] University of Texas, Arlington, Texas 76019, USA

[ca] Southern Methodist University, Dallas, Texas 75275, USA

[cb] Rice University, Houston, Texas 77005, USA

[cc] University of Virginia, Charlottesville, Virginia 22901, USA

[cd] University of Washington, Seattle, Washington 98195, USA

Abstract

We present a new method for modeling the hadronic recoil in $W \to \ell\nu$ events produced at hadron colliders. The recoil is chosen from a library of recoils in $Z \to \ell\ell$ data events and overlaid on a simulated $W \to \ell\nu$ event. Implementation of this method requires that the data recoil library describe the properties of the

3

measured recoil as a function of the true, rather than the measured, transverse momentum of the boson. We address this issue using a multidimensional Bayesian unfolding technique. We estimate the statistical and systematic uncertainties from this method for the W boson mass and width measurements assuming 1 fb^{-1} of data from the Fermilab Tevatron. The uncertainties are found to be small and comparable to those of a more traditional parameterized recoil model. For the high precision measurements that will be possible with data from Run II of the Fermilab Tevatron and from the CERN LHC, the method presented in this paper may be advantageous, since it does not require an understanding of the measured recoil from first principles.

Key words: W, Z, mass, width, hadron, collider, Tevatron, D0, recoil

PACS: 12.15.Ji, 13.85.Qk, 14.70.Fm, 12.38.Be

1. Introduction

The W and Z bosons are massive gauge bosons that, along with the massless photon, mediate electroweak interactions. The predictions from the standard model (SM) of weak, electromagnetic, and strong interactions [1] for their masses and widths include radiative corrections from the top quark and the Higgs boson. When precision measurements of the W boson mass (M_W) are combined with measurements of the top quark mass and other electroweak observables, limits on the Higgs boson mass can be extracted. The W boson width (Γ_W) can be directly measured from the fraction of W bosons produced at high mass. It can also be inferred indirectly within the context of the SM from the leptonic branching fraction of the W boson. The branching fraction, in turn, can be inferred from the ratio of the W and Z boson cross sections with additional theoretical inputs [2]. The direct measurement of Γ_W is sensitive to vertex corrections from physics beyond the SM. The current world average for M_W is 80.398 ± 0.025 GeV [3] and the current world average for Γ_W is 2.106 ± 0.050 GeV from direct measurements [4]. The large number of W bosons currently available in data samples collected at the Fermilab Tevatron collider and that will soon be available from the CERN LHC collider allow measurements of M_W and Γ_W with unprecedented precision provided the response of the detector can be modeled with sufficient accuracy.

In $p\bar{p}$ and pp collisions, W and Z bosons are produced predominantly through quark-antiquark annihilation. Higher order processes can include radiated gluons or quarks that recoil against the boson and

---

introduce non-zero boson transverse momentum [5]. Figure 1 shows an example diagram for the production of a W or Z boson with two radiated gluons in a $p\bar{p}$ collision.

We identify W and Z bosons through their leptonic decays ($W \to \ell\nu$ and $Z \to \ell\ell$ with $\ell = e, \mu$) since these signatures have low backgrounds. The charged leptons can be detected by the calorimeter or the muon system, while the neutrino escapes undetected. We do not reconstruct particles whose momentum vectors are nearly parallel to the beam direction, and therefore we only use kinematic variables in the transverse plane that is perpendicular to the beam direction. The neutrino transverse momentum vector $(\vec{p}_T^{\,\nu})$ is inferred from the missing transverse energy $(\vec{\not{E}}_T)$, which can be calculated using the transverse momenta of the charged lepton $(\vec{p}_T^{\,\ell})$ and the recoil system $(\vec{u}_T)$:

$$\vec{\not{E}}_T = -[\vec{p}_T^{\,\ell} + \vec{u}_T]. \tag{1}$$

We measure $\vec{u}_T$ by summing the observed transverse energy vectorially over all calorimeter cells that are not associated with the reconstructed charged lepton.

The recoil system is difficult to model from first principles; unlike the decay lepton, it is a complicated quantity involving many particles, as well as effects related to accelerator and detector operation. The recoil system is a mixture of the "hard" recoil that balances the boson transverse momentum and "soft" contributions, such as particles produced by the spectator quarks (the "underlying event"), other $p\bar{p}$ (pp) collisions in the same bunch crossing, electronics noise, and residual energy in the detector from previous bunch crossings ("pileup"). Figure 2 shows transverse energies recorded in the calorimeter of the D0 detector versus azimuthal angle and pseudorapidity [6] for a typical $W \to e\nu$ candidate. The diffuse energy deposits spread over much of the detector are due to the recoil system.

The various components of this measured recoil system have different dependences on instantaneous luminosity. For example, pileup and additional inelastic collisions scale with instantaneous luminosity, while the contribution from the underlying event is luminosity independent. Moreover, detector effects such as suppression of calorimeter cells with low energy to minimize the event size (zero-suppression cuts) can introduce correlations between the calorimeter response to the hard component and various soft components in the event, so that the detector responses to these components cannot be modeled independently.

Two approaches have been used previously to model the W boson event, including the recoil system. One method takes the underlying physics from a standard Monte Carlo (MC) event generator and smears it parametrically to reproduce detector effects [3, 7, 8, 9]. The parameters are tuned to an independent but kinematically similar data set, namely $Z \to \ell\ell$ events. The second approach, or "Ratio Method", constructs M_T template distributions by directly taking $Z \to \ell\ell$ events from collider data, treating one of the leptons as a neutrino [10]. The ratio of the Z boson mass to the corresponding W boson mass, taken together with the precisely measured Z boson mass [11] from the CERN LEP collider determines the W boson mass. In this method, small differences in the Z and W boson line shapes and transverse momentum and rapidity

distributions of the decay leptons must be taken into account.

This paper presents a novel approach for modeling the recoil system in $W \to \ell\nu$ events at hadron colliders that uses recoils extracted directly from $Z \to \ell\ell$ collider data. The $Z \to \ell\ell$ data provide a mapping between the Z boson transverse momentum $(\vec{p}_T^{\,Z})$ and the transverse momentum of the recoil system $(\vec{u}_T)$. Versions of the recoil library approach have been proposed in the past [12] that used the map between the reconstructed $\vec{p}_T^{\,Z}$ and the measured $\vec{u}_T$ directly. In this paper we use a two-dimensional Bayesian unfolding method to derive a relation between the true $\vec{p}_T^{\,Z}$ and the measured $\vec{u}_T$, which allows the simulation of the recoil system for the same generator level value of the W boson transverse momentum $(\vec{p}_T^{\,W})$.

The recoil library method presented in this paper has many advantages. Since the recoils are taken directly from $Z \to \ell\ell$ data, they reflect the event-by-event response and resolution of the detector. The additional soft recoil is built in, as is the complicated zero-suppression-induced correlations between it and the hard component of the recoil. Proper scaling of the recoil system with instantaneous luminosity is automatic since the W and Z samples have similar instantaneous luminosity profile. The most significant advantage of this method lies in its simplicity since it does not require a first-principles understanding of the recoil system and has no adjustable parameters. The dominant systematic uncertainties of this approach come from the limited statistical power of the $Z \to \ell\ell$ recoil library, as is true with the other methods.

In this paper, we outline the implementation of this method. The method is tested using the W boson mass and width measurements. Only the electron decay channel is discussed, but our method can also be used in the muon decay channel. The detector and selection criteria are described in Section 2. The MC simulation samples used are described in Section 3. We discuss the method in Section 4. In Sections 5 and 6, we assess the uncertainty on the W boson mass and width measurements, and compare the performance of this method with that of a parameterized recoil model. The paper concludes in Section 7.

2. The W and Z Boson Measurements

We evaluate the recoil library method by estimating biases and statistical and systematic uncertainties on the W boson mass and width measurements in the electron channel. The test is performed using simulations of the Run II D0 detector at the Fermilab Tevatron, a $p\bar{p}$ collider with center of mass energy $\sqrt{s} =1.96$ TeV. Statistical uncertainties are estimated for a data sample corresponding to 1 fb^{-1}.

2.1. The D0 Detector

The D0 detector [13, 14] consists of a magnetic central-tracking system, comprised of a silicon microstrip tracker (SMT) and a central fiber tracker (CFT), both located within a 2 T superconducting solenoidal magnet. The SMT and CFT cover $|\eta_D| < 3.0$ [6] and $|\eta_D| < 1.8$, respectively.

Three uranium/liquid argon calorimeters measure particle energies. The central calorimeter (CC) covers $|\eta_D| < 1.1$, and two end calorimeters (EC) extend coverage to $|\eta_D| \approx 4.2$. In addition to the preshower

detectors, scintillators between the CC and EC cryostats provide sampling of developing showers at $1.1 < |\eta_D| < 1.4$. The CC is segmented in depth into eight layers. The first four layers are used primarily to measure the energies of photons and electrons and are collectively called the electromagnetic (EM) calorimeter. The remaining four layers, along with the first four, are used to measure the energies of hadrons. Most layers are segmented into 0.1×0.1 regions in (η, ϕ) [6] space. The third layer of the EM calorimeter is segmented into 0.05×0.05 regions.

A muon system is located beyond the calorimetry and consists of a layer of tracking detectors and scintillator trigger counters before 1.8 T iron toriods, followed by two similar layers after the toroids. Tracking at $|\eta_D| < 1$ relies on 10 cm wide drift tubes, while 1 cm mini-drift tubes are used at $1 < |\eta_D| < 2$.

Scintillation counters covering $2.7 < |\eta_D| < 4.4$ are used to measure luminosity and to indicate the presence of an inelastic collision in beams crossing.

2.2. Measurement strategies for M_W and Γ_W

The W boson mass is measured from distributions of the following observables: the electron transverse momentum $\vec{p}_T^{\,e}$, the missing transverse energy $\vec{\not{E}}_T$, and the transverse mass M_T, given by

$$M_T = \sqrt{2|\vec{p}_T^{\,e}|\ |\vec{\not{E}}_T|[1 - \cos(\Delta\phi)]}, \tag{2}$$

where $\Delta\phi$ is the opening angle between $\vec{p}_T^{\,e}$ and $\vec{\not{E}}_T$ in the transverse plane. The data distributions are compared with probability density functions from MC simulations generated with various input W boson mass values ("templates"). A binned negative log-likelihood method is used to extract M_W. The W boson width is measured using a similar method, except that only events in the high tail region of the M_T distribution are used. For the mass measurement, the fit ranges we used are [30, 48] GeV for the $|\vec{p}_T^{\,e}|$ and $|\vec{\not{E}}_T|$ distributions, and [60, 90] GeV for the M_T distribution. For the width measurement, we fit the M_T distribution over the range [100, 200] GeV.

2.3. Selection criteria

A W boson candidate is identified as an isolated electromagnetic cluster accompanied by large $|\vec{\not{E}}_T|$. The electron candidate is required to have a shower shape consistent with that of an electron, $|\vec{p}_T^{\,e}| > 25$ GeV, and $|\eta_D| < 1.05$. To further reduce backgrounds, the electron candidate is required to be spatially matched to a reconstructed track in the central tracking system. Additionally, we require $|\vec{\not{E}}_T| > 25$ GeV, $|\vec{u}_T| < 15$ GeV, and $50 < M_T < 200$ GeV. Z boson candidates are identified as events containing two such electrons with di-electron invariant mass $70 < M_{ee} < 110$ GeV and $|\vec{u}_T| < 15$ GeV. The selection on $|\vec{u}_T|$ helps to suppress background and to reduce the sensitivity of the measurement to uncertainties on the detector model and the theoretical description of the p_T^W distribution. Since the Z sample has fewer events at high p_T^Z, the detector and theoretical models are best constrained at low boson p_T.

7

For this analysis, both electrons from the Z boson are required to be in the central region of the calorimeter because the unfolding requires well-understood detector resolutions.

3. MC Simulation Samples

In this paper we use three different MC simulations. Two of these are fast MC simulations and the third is a detailed full MC simulation using GEANT [15]. The two fast MC simulations are built around a common event generator and parametric model for the electron measurement, but with different recoil models. One uses a traditional parameterized method to model the recoil system, which we call "the parameterized recoil method". The other uses our new method, which we call "the recoil library method". The full MC $Z \rightarrow ee$ sample has the equivalent of 6.0 fb^{-1} in integrated luminosity, and the full MC $W \rightarrow e\nu$ sample corresponds to 2.5 fb^{-1}.

For both fast MCs, the PYTHIA [16] event generator is used to simulate the production and decay of the W boson, as well as any final state radiation (FSR) photons. FSR photons, if sufficiently close to the electron, are merged with the electron. After the event kinematics are generated at the four-vector level, detector efficiencies and energy response and resolution for the electron are applied. These parameterizations are measured using $Z \rightarrow ee$ events from either collider data or full MC, depending on the study. A parametric energy dependent model for resolution effects is used. Parameterized efficiencies for data selection are prepared for comparing with either data or full MC as a function of electron $|\vec{p}_T^e|$, η^e, the component of the recoil along the electron direction, the total hadronic activity in the event, and the reconstructed z coordinate along the beam line where the hard scattering occurred. The recoil system is then modeled either using the recoil library or the parameterized model.

The parameterized recoil method models the detector response to the hard recoil using a two-dimensional parameterization of the response (both magnitude and direction) as estimated using GEANT-simulated $Z \rightarrow \nu\bar{\nu}$ events. The underlying event is modeled using the measured $\vec{\rlap{/}{E}}_T$ distribution from data taken with a trigger that requires energy in the luminosity monitors ("minimum bias events"), and pileup and additional interactions are modeled using the measured $\vec{\rlap{/}{E}}_T$ distributions from unsuppressed data taken on random beam crossings ("zero bias events"). These are combined with the hard recoil, and data-tuned corrections are applied to account on average for correlations between the "hard" and "soft" recoil. The correction parameters are tuned to $Z \rightarrow ee$ control samples. The parametric methods of modeling the recoil are further discussed in Refs. [17] and resemble approaches used in earlier D0 and CDF measurements at the Tevatron [3, 8, 9]. The recoil library method of modeling the recoil is discussed in detail in Section 4.

The GEANT-based MC simulation also uses PYTHIA to simulate the production and decay of the W boson, as well as the underlying event and any FSR photons. These events are then propagated through a detailed description of the detector. Zero bias collider data collected by the D0 detector with a similar

8

instantaneous luminosity profile as the $W \to e\nu$ collider data sample are overlaid on the full MC simulation to model additional collisions and noise in the detector. These events are processed through the same full set of D0 reconstruction programs as data.

4. The Recoil Library Method

4.1. Overview

The recoil library is built from $Z \to ee$ events. Because the electron energies and angles are well measured, the measured $\vec{p}_T^Z$ from the two electrons provides a good first approximation of the true $\vec{p}_T^Z$. An unfolding procedure allows the transformation of the two-dimensional distribution of the measured $|\vec{p}_T^Z|$ and measured $|\vec{u}_T|$ to that of the true $|\vec{p}_T^Z|$ and measured $|\vec{u}_T|$. The opening angle between the measured $\vec{p}_T^Z$ and the measured $\vec{u}_T$ is also unfolded to the opening angle between the true $\vec{p}_T^Z$ and the measured $\vec{u}_T$ during this procedure. A map between the true $|\vec{p}_T^Z|$, the measured $|\vec{u}_T|$, and the scalar E_T (SE_T), which is defined as the scalar sum of the transverse energies of all calorimeter cells except those that belong to the reconstructed electrons, is also produced. This map is not used by the recoil model, but is needed by the electron efficiency model. The final result of the recoil library is the $\vec{u}_T$ for an event, referenced to the true $\vec{p}_T^Z$. This vector substitutes for the equivalent vector obtained in the parametrized recoil model. All further corrections for efficiencies due to the recoil system are the same for both the recoil library and the parametrized recoil model.

Figure 3 shows some examples of the distribution of the component of the measured recoil along the Z boson direction and perpendicular to the Z boson direction.

4.2. Preparing the recoil library

Before producing a binned recoil library, certain event-by-event corrections must be applied to the measured recoil system. We need to remove any biases in the measured recoil distribution due to the Z boson selection requirements. Electron identification requirements, for example, preferentially reject events with significant hadronic activity. Events with significant hadronic activity also have poorer recoil resolution than events with little hadronic activity. Since Z bosons contain two electrons while W bosons only have one, the bias will not be the same. The electrons from Z boson decays also have a higher average $|\vec{p}_T^e|$ and a different η^e distribution than electrons from W boson decays. To account for this, we remove the biases from the Z boson selection, and then, when a W candidate is made using the recoil library, the biases appropriate for a W candidate are added, as described in Ref. [17]. In this section, we describe these corrections to the Z boson sample.

4.2.1. Removing the two electrons from Z boson events

The recoil system for $Z \to ee$ events is defined as the energies in all calorimeter cells excluding those that belong to the two electrons. Since the recoil system will in general deposit energy in these cells, excluding them biases the component of the recoil along the electron's direction. We correct this effect by adding back an approximation of the underlying energy.

This correction (denoted by $\Delta u_\parallel^e$) depends on $u_\parallel^e$ (the projection of $\vec{u}_T$ along the electron transverse direction), instantaneous luminosity, and electron η^e, and is estimated using the energies deposited in equivalent cells that are separated in ϕ from the electron in $W \to e\nu$ events. In addition to correcting for the recoil energy under the electron cluster, we also correct for electron energy that leaks out of the cluster. For Z boson events, these corrections are made for both electrons. In Section 5 we estimate the uncertainty due to these corrections.

4.2.2. Minimizing the effects of FSR photons

The full MC simulation indicates that roughly 6% of the $Z \to ee$ events contain FSR photons with $E_T^\gamma > 400$ MeV that are sufficiently far from the electrons that the electron clustering algorithm at D0 does not merge them with a reconstructed electron. These photons are thus incorrectly included in the measurement of $\vec{u}_T$, instead of in $\vec{p}_T^Z$, resulting in a correlated bias. Since $Z \to ee$ events contain more FSR photons than $W \to e\nu$ events do, the recoil library built using Z bosons will contain on average larger contributions from FSR photons.

Ideally, these FSR photons could be removed from the recoil file, and the effect could be separately modeled within the fast MC simulation. Since it is difficult to identify these FSR photons on an event-by-event basis, the effect is reduced by raising the lower limit on the effective reconstructed di-electron invariant mass to 85 GeV, reducing the fraction of events with a high E_T FSR photon by 25%.

The effect of the remaining photons is small because, for a low p_T W boson, $M_T \approx 2|\vec{p}_T^e| + u_\parallel^e$. Therefore, the photons will create a bias on the mass only if they produce a bias in the component of $\vec{u}_T$ parallel to the electron direction. While the overlaid recoil is rotated so that the direction of its corresponding Z boson matches that of the simulated W boson, the directions of the decay electrons from Z and W are largely uncorrelated, and the bias is mostly canceled for measurements using the M_T spectrum. In Section 5 the bias due to the FSR photons is estimated.

4.2.3. Correcting for electron selection efficiencies

The selection criteria for W and Z candidates can introduce biases between the electron and the recoil system. Since the kinematic and geometric properties of W candidates are not identical to those of Z candidates, they have different biases.

The two components of the electron selection efficiency model that most strongly affect these biases are

the SE_T efficiency and the $u_\parallel^e$ efficiency. The SE_T efficiency describes the electron identification probability as a function of the overall activity in the detector. The $u_\parallel^e$ efficiency describes the probability of electron identification as a function of $u_\parallel^e$. This probability decreases with increasing hadronic activity along the electron direction.

Since the recoil library is built from $Z \to ee$ events, we need to remove the biases introduced by the selection requirements on the two electrons. We correct for the efficiencies by weighting each event in the Z boson recoil library by $1/\epsilon_{u_\parallel^e} \times 1/\epsilon_{SE_T}$, where $\epsilon_{u_\parallel^e}$ is the product of the $u_\parallel^e$ efficiencies and ϵ_{SE_T} is the product of the SE_T efficiencies for the two electrons in each Z candidate.

When W boson events are produced from a fast MC using the recoil library, the map between the true $\vec{p}_T^Z$, measured $\vec{u}_T$, and SE_T is used to introduce the biases appropriate for W bosons from these efficiencies. To simulate a W boson event, a random recoil is chosen from the recoil library corresponding to the true W boson p_T^W, and a random SE_T is chosen from the SE_T distribution corresponding to the true W boson p_T^W and the chosen recoil $\vec{u}_T$. The $u_\parallel^e$ efficiency and SE_T efficiency are then applied to the electron from W boson decays.

4.3. Unfolding method

After the recoils have been corrected as discussed above, the transformation from measured $\vec{p}_T^Z$ and measured $\vec{u}_T$ to true $\vec{p}_T^Z$ and measured $\vec{u}_T$ is done using a Bayesian unfolding technique.

4.3.1. Multidimensional unfolding using Bayes's Theorem

Unfolding is a mathematically challenging problem, since it involves the reversal of a random process. Because a given true state can migrate to many measured states and many different true states can migrate to the same measured state, we cannot unfold detector effects on an event-by-event basis. Rather, unfolding methods typically work with binned distributions.

For the recoil library method, we chose to use a Bayesian unfolding approach [18]. This approach suits our needs because it is intuitive, simple to implement, and easy to extend to the multidimensional case. The Bayesian technique uses conditional probabilities to determine the probability that a given measured state corresponds to a particular true state.

Consider a distribution of initial states I_i, $\{i = 1, 2, ..., N_I\}$, given by $P(I_i)$ (the probability of events with initial state I_i) and a distribution of final states F_j, $\{j = 1, 2, ..., N_F\}$, given by $P(F_j)$ (the probability of events with final state F_j), given the measured distribution $P(F_j)$, and the probability for each initial state to migrate to each final state $P(F_j|I_i)$, we can determine the distribution of initial states $P(I_i)$ using

$$P(I_i) = \sum_{j=1}^{N_F} P(I_i|F_j)P(F_j). \tag{3}$$

11

Using simulations, we can calculate $P(I_i|F_j)$ from $P(F_j|I_i)$, the likelihood of a true state fluctuating to a measured state, using Bayes's theorem, which is

$$P(A|B) = \frac{P(B|A)P(A)}{P(B)}. \tag{4}$$

For our particular example, with N_I initial states and N_F final states, Bayes's theorem gives us

$$P(I_i|F_j) = \frac{P(F_j|I_i)P(I_i)}{\sum_{k=1}^{N_I} P(F_j|I_k)P(I_k)}. \tag{5}$$

We can interpret this equation as follows: the probability that a given final state F_j comes from a particular initial state I_i is proportional to the probability density of state I_i multiplied by the probability that I_i migrates to F_j. The denominator normalizes the distribution.

Our Bayesian method requires us to make assumptions regarding the distribution of initial states, $P(I_i)$. Although we only use $P(I_i)$ to calculate the weights used for the measured data, the quality of the unfolding could depend on $P(I_i)$. To minimize this effect, the method is applied iteratively, starting with a reasonable prior for the distribution with $P_0(I_i)$, and with each successive iteration using the previous iteration's unfolded distribution as the new input. As a cross-check, the method is applied with several different initial $P_0(I_i)$ distributions. The iteration procedure is:

1. Choose an initial seed input distribution for $P_0(I_i)$.

2. Using $P_0(I_i)$ and $P(F_j|I_i)$, compute the weights $P(I_i|F_j)$, as derived using the Bayesian equation shown in Eq. 5.

3. Using these weights, recalculate the unfolded distribution $P_1(I_i)$ from the relationship $P_1(I_i) = \sum_{j=1}^{N_F} P_0(F_j)P(I_i|F_j)$ described in Eq. 3.

4. Repeat the above steps with $P_1(I_i)$ as the starting distribution.

5. Iterate until the unfolded $P(I_i)$ converges.

4.3.2. Unfolding the recoil distribution

For our application, the recoil vector is described by the coordinates $(|\vec{u}_T|, \psi^t)$, where $|\vec{u}_T|$ is the magnitude of the measured recoil transverse momentum, and ψ^t is the opening angle between the measured recoil and the true boson direction in the transverse plane. These recoil vectors are stored in an array of two-dimensional recoil histograms (binned in $|\vec{u}_T|$ and ψ^t). Each histogram corresponds to a discrete bin in true $|\vec{p}_T^Z|$ with bins of 0.25 GeV for small $|\vec{p}_T^Z|$ ($|\vec{p}_T^Z| < 50$ GeV) and larger bins at larger $|\vec{p}_T^Z|$.

In the implementation of Eq. 5, the initial state I is specified by $[(|\vec{p}_T^Z|)_i^t, \psi_j^t, (|\vec{u}_T|)_k]$ and the final state F is given by $[(|\vec{p}_T^Z|)_m^s, \psi_n^s, (|\vec{u}_T|)_k]$, where $(|\vec{p}_T^Z|)^t$ is the true Z boson transverse momentum, $(|\vec{p}_T^Z|)^s$ is the smeared Z boson transverse momentum, and ψ^s is the opening angle between the measured recoil and the smeared Z boson direction in the transverse plane.

We start with an initial seed distribution that is flat in $(|\vec{p}_T^Z|)^t$, ψ^t, and $|\vec{u}_T|$. We find that it takes fewer than 10 iterations for the unfolding method to converge. Figure 4 shows the convergence of the W boson mass and width obtained from the M_T distribution, as a function of iteration number in fast MC studies. The final value achieved agrees well with the input value. The systematic uncertainty on the W boson mass and width due to the unfolding procedure is discussed further in Section 5.

Figure 5 shows an example distribution of the probabilities that a Z boson with a reconstructed $|\vec{p}_T^Z|$ of 7 GeV and a recoil $|\vec{u}_T|$ of 3.5 GeV corresponds to different true $|\vec{p}_T^Z|$ values. These probabilities are used to weight the given recoil as we store it in the recoil histograms corresponding to the true $|\vec{p}_T^Z|$. Figures 6–10 show various recoil observables plotted versus the true $|\vec{p}_T^Z|$, obtained from the truth information of these MC samples, compared with the same observables plotted versus the reconstructed $|\vec{p}_T^Z|$, before and after the unfolding is applied. The unfolding corrects for average effects of $|\vec{p}_T^Z|$ smearing on both the means and the RMS values of these recoil observables.

5. Uncertainties Particular to the Recoil Library Method

To perform high statistics tests of the efficacy of the recoil library, we study the mass and width values obtained by comparing $|\vec{p}_T^e|$, $|\vec{\not{E}}_T|$ and M_T distributions obtained from fast MC W boson samples created using the parameterized recoil model with templates generated from W boson samples created using the recoil library method. The recoil libraries are generated from $Z \to ee$ events created with the parameterized recoil method. By varying parameters in the simulation used to generate the W boson samples while leaving the templates unchanged, we measure the biases and statistical and systematic uncertainties on the recoil library method for $p\bar{p}$ collisions at $\sqrt{s} = 1.96$ TeV. The corresponding uncertainties for W boson mass and width measurements at the LHC remain to be evaluated, but are not expected to be large.

5.1. Statistical power of the Z recoil sample

There are significant statistical uncertainties since we obtain the recoil system for modeling the $W \to e\nu$ events from the limited sample of Z boson events. In 1 fb^{-1} of data, after the selection cuts, we expect approximately 18,000 $Z \to ee$ events with both electrons in the central calorimeter, whereas in the same data we expect approximately 500,000 $W \to e\nu$ events with the electron in the central calorimeter. For the recoil library method, we choose recoil vectors from the same set of 18,000 $Z \to ee$ events to make W boson templates. Our method is thus limited by the size of the Z recoil sample and any statistical fluctuations it contains. If we are to rely on this method as an input to a precision measurement, we need to determine the extent to which the statistical limitations of the $Z \to ee$ sample propagate to an uncertainty on the measured W boson mass and width.

We assess the statistical uncertainties of the recoil method using an ensemble of 100 fast MC simulations resembling the statistical situation we expect in real data. We generate W and Z boson samples corresponding to 1 fb^{-1} of data using the parameterized recoil method. For each set of W and Z boson samples, we use the Z boson events to create a recoil library and then use the library to create templates for the recoil in the simulated W boson events. These templates are then used to extract the W boson mass and width. The statistical power is measured using the spread of extracted masses and widths from these ensembles.

Figure 11 shows the measured W boson masses and widths from 100 ensembles using the M_T distribution. The mean fit value is in good agreement with the input value, showing that the recoil library can accurately model the parameterized recoil method. We test that the recoil library can model the full MC events in Section 6.

The statistical uncertainty on the mass measurement due to the recoil library method is found to be 5 MeV from the M_T spectrum, 8 MeV for the $|\vec{p}_T^{\,e}|$ spectrum, and 17 MeV for the $|\vec{\not{E}}_T|$ spectrum. These agree with the statistical uncertainties on the parameterized recoil method, which are found to be 6 MeV for the M_T fit, 7 MeV for the $|\vec{p}_T^{\,e}|$ fit, and 19 MeV for the $|\vec{\not{E}}_T|$ fit. The statistical uncertainty on the width measurement due to the recoil library method is 40 MeV using the M_T spectrum and agrees with the statistical uncertainty of 42 MeV using the parameterized recoil method.

Both the parameterized recoil and the recoil library methods use the Z boson sample to model the recoil. One might naively expect that the additional information contained in the functional form used in the parameterized method would give it increased statistical power for the same-sized sample. However, we do not observe a loss of statistical power since the uncertainties from the two methods are very similar to each other. We have explored the reason for this by using a simplified detector model of W and Z boson events with and without recoil energy resolution effects added, and comparing the p_T-imbalance (the difference between $|\vec{p}_T^{\,Z}|$ and the projection of the recoil $\vec{u}_T$ along the boson direction) distribution for the parameterized and library methods. Due to the similar transverse momentum distributions of the W and Z bosons, we find that the means of the p_T-imbalance distribution agree with each other within statistical uncertainty. We also find that without recoil energy resolution effects, there is a clear but small, $\mathcal{O}(100)$ MeV, increase in the RMS of the p_T-imbalance distributions for the recoil library method, but with the detector resolution effects added, the RMS of the p_T-imbalance distribution increases to over 2 GeV and masks any difference stemming from the difference between the parameterized recoil method and the recoil library method.

5.2. Systematic uncertainties

We mentioned in Section 4 that several effects could potentially bias the recoil library method. These include unmerged FSR photons, acceptance differences between Z and W boson events, residual efficiency-related correlations between the electron and the recoil system, underlying energy corrections beneath the

electron window, and the unfolding process. The closure tests using fast MC described in Section 5.1 show the overall bias from this method to be smaller than the statistical power of the tests. Nonetheless, we want to make sure that this small final bias is not due to the cancellation of larger individual biases and therefore examine each effect independently.

5.2.1. Unmerged FSR photons

We measure the residual bias due to FSR photons by fitting two sets of fast MC simulations, one made from an unfolded, high statistics recoil file with all FSR photons included and one made from an equivalent recoil file with no FSR photons. We find that the mass shift between these two samples is -1 MeV for the M_T fit, -2 MeV for the $|\vec{p}_T^{\,e}|$ fit, and 2 MeV for the $|\vec{\rlap{/}E}_T|$ fit, and that the width shift is less than 1 MeV.

5.2.2. Differences in geometric acceptance

For W candidates, we only require the electron to be in the central calorimeter, while for Z candidates used to create the library, we require both electrons to be in the central calorimeter. To test the bias due to this effect, we generate two recoil files. For one recoil file we restrict both electrons to the central region of the detector, as we would in data. For the other recoil file, we restrict only one electron to the central calorimeter and allow the other electron to be anywhere, as with the neutrino from the W boson decay. We make templates from the two recoil files and find that the differences in both measured mass and measured width are smaller than the 2 MeV statistical uncertainty of this study.

5.2.3. Efficiency related biases

When we generate unfolded recoil files, we weight the events by the reciprocals of the $u_\parallel^e$ and SE_T efficiencies, as described in Section 4.2.3. To check if this approach introduces any biases, we perform three tests. For one, we only apply the $u_\parallel^e$ efficiency. In the second test, we only apply the SE_T efficiency, and in the final test we apply both efficiencies. The maximum bias in the fitted mass or width over all three tests is used as the systematic uncertainty. The final uncertainty attributed to the efficiency corrections on the W boson mass is 7 MeV for the M_T fit, 7 MeV for the $|\vec{p}_T^{\,e}|$ fit, and 8 MeV for the $|\vec{\rlap{/}E}_T|$ fit. The uncertainty of the W boson width is found to be 7 MeV.

5.2.4. Uncertainty in $\Delta u_\parallel^e$

In Section 4.2 we observed that by removing the electrons from the $Z \rightarrow ee$ recoil file, we also remove the recoil energy that underlies the electron cones. We correct for this effect by adding back the average energy, $\Delta u_\parallel^e$, expected beneath the electrons. We then subtract the electron energy that leaks outside of the electron cone that is incorrectly attributed to the recoil energy.

We assess the systematic uncertainty due to these corrections as follows. Z boson recoil files are made for three cases: (1) no energy corrections, (2) a constant energy correction for underlying hadronic energy

beneath the electron cone and constant correction for the electron energy leakage, (3) the parameterized energy correction for underlying hadronic energy beneath the electron cone and constant correction for the electron energy leakage.

We then generate three sets of templates from each of these recoil files and measure the shift in fitted W boson mass and width between these three template sets. The W boson mass shifts by 2 MeV for the M_T fit, 4 MeV for the $|\vec{p}_T^{\,e}|$ fit, and 1 MeV for the $|\vec{\not{E}}_T|$ fit, with a 7 MeV shift for the width. We assign the magnitude of these maximum shifts as the uncertainty on this method due to the $\Delta u_\parallel^e$ correction.

5.2.5. Uncertainties due to implementation of unfolding

The specific choices made in implementing the unfolding could introduce biases to the final measurement. Our results may depend on our choice of initial distributions in $(|\vec{p}_T^{\,Z}|)^t$, ψ, and $|\vec{u}_T|$. They could also depend on the number of iterations of the unfolding procedure we apply to the recoil library.

We find that starting with flat initial distributions in $(|\vec{p}_T^{\,Z}|)^t$, ψ, and $|\vec{u}_T|$, ten iterations are sufficient to attain convergence. We generate the unfolded recoil files using 8, 10, and 12 iterations of the unfolding method and find that the changes in measured mass and width extracted from M_T, $|\vec{p}_T^{\,e}|$, and $|\vec{\not{E}}_T|$ fits are within 3 MeV statistical uncertainty of the fast MC study. In addition to unfolding the recoil file using a flat initial distribution for the recoil spectrum, we also try several smoothly varying sinusoidal initial distributions, and find that the variation in the final unfolded recoil file is negligible.

5.3. Total systematic uncertainties due to the recoil system simulation

Table 1 shows the estimated systematic uncertainties due to the recoil system simulation for 1 fb^{-1} of fast MC data. The overall systematic uncertainties, obtained by adding the individual uncertainties in quadrature, are found to be 9 MeV using the M_T fit, 12 MeV using the $|\vec{p}_T^{\,e}|$ fit, and 19 MeV using the $|\vec{\not{E}}_T|$ fit for the W boson mass, and 41 MeV using the M_T fit for the W boson width.

6. Full MC closure of W boson mass and width

We test both the recoil library method and the parameterized recoil method using a detailed MC sample produced using a GEANT-based full detector model for W and Z boson production. The full MC Z boson sample is equivalent to 6.0 fb^{-1} and the W boson sample is equivalent to 2.5 fb^{-1}. In this case, the full MC Z boson samples are used to create the recoil library. Templates are then created from W boson samples made using the recoil library, and these are used to extract the W boson mass and width. The extracted values for the W boson mass and width are compared to the input values (closure test).

Before fitting for the mass and width of the full MC sample, we test the accuracy of the model by comparing various full MC distributions to the fast MC model for an input value of the W boson mass of 80.450 GeV. Good agreement between full MC and fast MC using the recoil library method is observed.

Figure 12 shows comparisons between $W \to e\nu$ full MC and fast MC using the recoil library method for the M_T, $|\vec{p}_T^{\,e}|$, and $|\vec{\not{E}}_T|$ distributions. The χ^2 between full and fast MC simulations are also given and are reasonable. The systematic uncertainties on the electron model, dominated by the uncertainty on the electron energy scale, are found to be 15 MeV for the M_T and $|\vec{\not{E}}_T|$ fits, and 12 MeV for the $|\vec{p}_T^{\,e}|$ fit for the W boson mass, and 15 MeV for the W boson width. Systematic uncertainties on the hadronic model are taken from Section V. Since here we use the equivalent of 6.0 fb^{-1} of full MC $Z \to ee$ recoils, we estimate the overall uncertainty due to the recoil system simulation by scaling the uncertainty due to recoil statistics found in Section V by a factor of $1/\sqrt{6}$, leaving other estimated systematic uncertainties the same. The systematic uncertainty due to the recoil statistics is 2 MeV using the M_T fit, 3 MeV using the $|\vec{p}_T^{\,e}|$ fit, and 7 MeV using the $|\vec{\not{E}}_T|$ fit for the W boson mass and 16 MeV using the M_T fit for the W boson width, which agrees with the corresponding systematic uncertainty in the parameterized recoil model. Taking the systematic uncertainties estimated in Section V, added in quadrature with these statistical uncertainties, we find the total uncertainty to be 22 MeV for the M_T fit, 24 MeV for the $|\vec{p}_T^{\,e}|$ fit and 26 MeV for the $|\vec{\not{E}}_T|$ fit for the W boson mass, and 36 MeV for the W boson width.

The results of the full MC measurements agree with the full MC input W boson mass and width values within the uncertainties, as shown in Table 2.

7. Conclusion

We have outlined a method to model the hadronic recoil system in $W \to \ell\nu$ events using recoils extracted directly from a $Z \to \ell\ell$ data library. We applied this methodology to a realistic full MC simulation of the D0 detector. The W boson mass and width fits to these MC events are in good agreement with the input parameters, within statistical uncertainties. They also agree with the values extracted using a more traditional parameterized recoil model. Comparisons of simulated distributions using the recoil library method with MC give good χ^2 agreement over a full range of data observables.

This method is limited by the statistical power of the Z boson recoil sample, as is the parameterized recoil model. In addition to systematic effects from the limited statistical power of the Z boson sample, there are several systematic effects due to the implementation of the selection efficiencies, geometric acceptance, the unfolding method, and FSR. The uncertainty due to these effects is found to be $\mathcal{O}(10)$ MeV.

The method presented in this paper has many advantages. It accurately describes the highly complicated hadronic response and resolution for W boson recoils in a given calorimeter. It includes complex correlations between the hard and soft components of the recoil and scales the recoil appropriately with luminosity. It requires fewer assumptions, no first-principles description of the recoil system, and no adjustable parameters. At hadron collider experiments at the Run II Tevatron and the LHC, this approach to modeling the recoil system is complementary to the traditional parametric approach.

Acknowledgement

References

[1] S. Glashow, Nucl. Phys. **B22**, 579 (1961); S. Weinberg, Phys. Rev. Lett. **19**, 1264 (1967); A. Salam, in *Elementary Particle Theory*, edited by N. Svartholm (Almqvist and Wiksells, Stockholm, 1969), p. 367; W. Bardeen, H. Fritzsch, and M. Gell-Mann, in *Scale and Conformal Symmetry in Hadron Physics*, edited by R. Gatto (Wiley, New York, 1973), p. 139; D. Gross and F. Wilczek, Phys. Rev. D **8**, 3633 (1973); S. Weinberg, Phys. Rev. Lett. **31**, 494 (1973).

[2] P.B. Renton, Rep. Prog. Phys. **65**, 1271 (2002).

[3] T. Aaltonen *et al.* (CDF Collaboration) Phys. Rev. Lett. **99**, 151801 (2007); Phys. Rev. D **77**, 112001 (2008).

[4] T. Aaltonen *et al.* (CDF Collaboration), Phys. Rev. Lett. **100**, 071801 (2008).

[5] C. Balazs and C.-P. Yuan, Phys. Rev. D **56**, 5558 (1997).

[6] D0 uses a cylindrical coordinate system with the z axis directed along the beam axis in the proton direction. Angles θ and ϕ are the polar and azimuthal angles, respectively. Pseudorapidity is defined as $\eta = -\ln[\tan(\theta/2)]$ where θ is measured with respect to the interaction vertex. In the massless limit, η is equivalent to the rapidity $y = (1/2)\ln[(E+p_z)/(E-p_z)]$. η_D is the pseudorapidity measured with respect to the center of the detector.

[7] D. Glenzinski and U. Heintz, Annu. Rev. Nucl. Part. Sci. **50**, 207 (2000); A. Kotwal and J. Stark, Annu. Rev. Nucl. Part. Sci. **58**, 147 (2008).

[8] V.M. Abazov *et al.* (D0 Collaboration), Phys. Rev. D **58**, 092003 (1998); B. Abbott *et al.* (D0 Collaboration), Phys. Rev. D **58**, 012002 (1998); B. Abbott *et al.* (D0 Collaboration), Phys. Rev. D **62**, 092006 (2000); V.M. Abazov *et al.* (D0 Collaboration), Phys. Rev. D **66**, 012001 (2002).

[9] T. Affolder *et al.* (CDF Collaboration), Phys. Rev. D **64**, 052001 (2001).

[10] D.L. Shpakov, Ph.D. thesis, State University of New York at Stony Brook (2000).

[11] C. Amsler *et al.*, Phys. Lett. B **667**, 1 (2008) and references therein.

[12] D.P. Saltzberg, Ph.D. thesis, Enrico Fermi Institute, University of Chicago (1994).

[13] S. Abachi *et al.* (D0 Collaboration), Nucl. Instrum. Methods Phys. Res., Sect. A **338**, 185 (1994).

[14] V.M. Abazov *et al.* (D0 Collaboration), Nucl. Instrum. Methods Phys. Res., Sect. A **565**, 463 (2006).

[15] R. Brun and F. Carminati, CERN Program Library Long Writeup W5013, 1993 (unpublished).

[16] T. Sjőstrand, S. Mrenna and P. Skands, JHEP **0605**, 026 (2006).

[17] V.M. Abazov *et al.* (D0 Collaboration), D0 Note 5893-CONF, to be submitted to Phys. Rev. Lett.

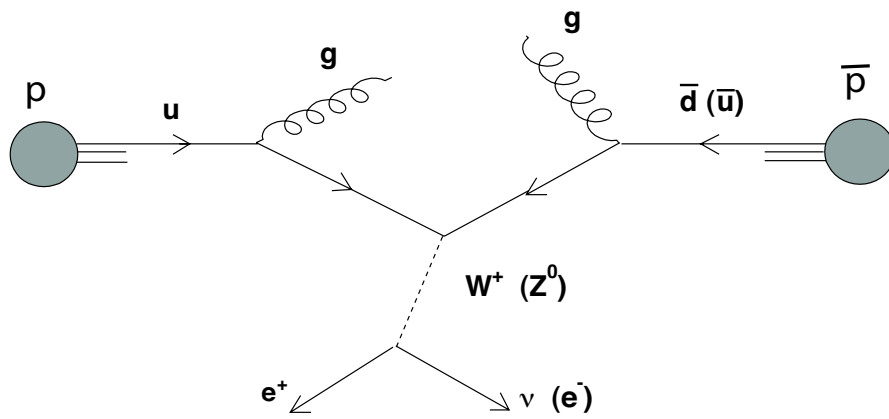[18] G. D'Agostini, Nucl. Instrum. Methods Phys. Res., Sect. A **362**, 487 (1995).

Figure 1: An example of a diagram for the production and leptonic decay of a W/Z boson with radiated gluons in a hadronic collision.
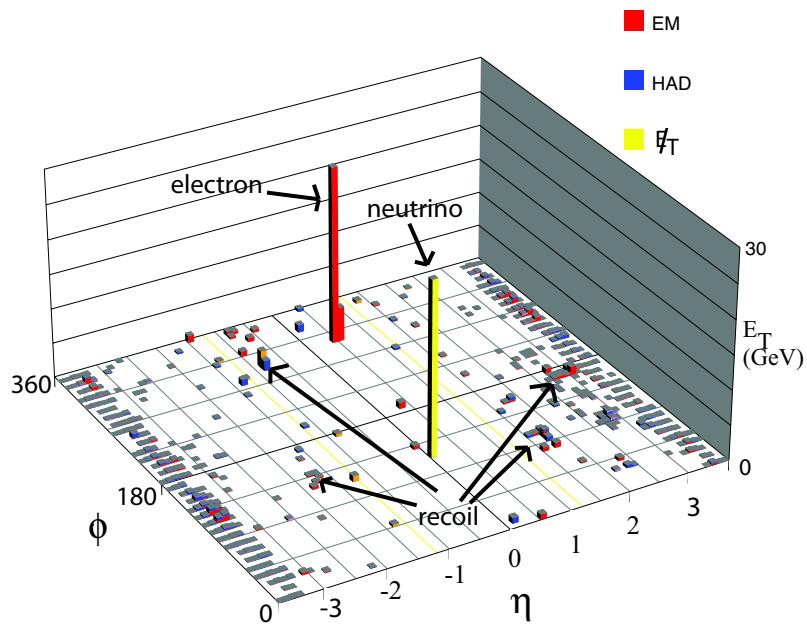
Figure 2: A typical $W \rightarrow e\nu$ candidate as recorded by the D0 detector. The x and y axes correspond to azimuthal angle and pseudorapidity, and the vertical axis is the transverse energy deposited at that location in the calorimeter. The energy associated with the electron and the $\vec{\not{E}}_T$ that corresponds to the neutrino are indicated. All other energies contribute to the measured recoil. The longitudinal component of the neutrino momentum is not determined, so it is displayed arbitrarily at $\eta = 0$.
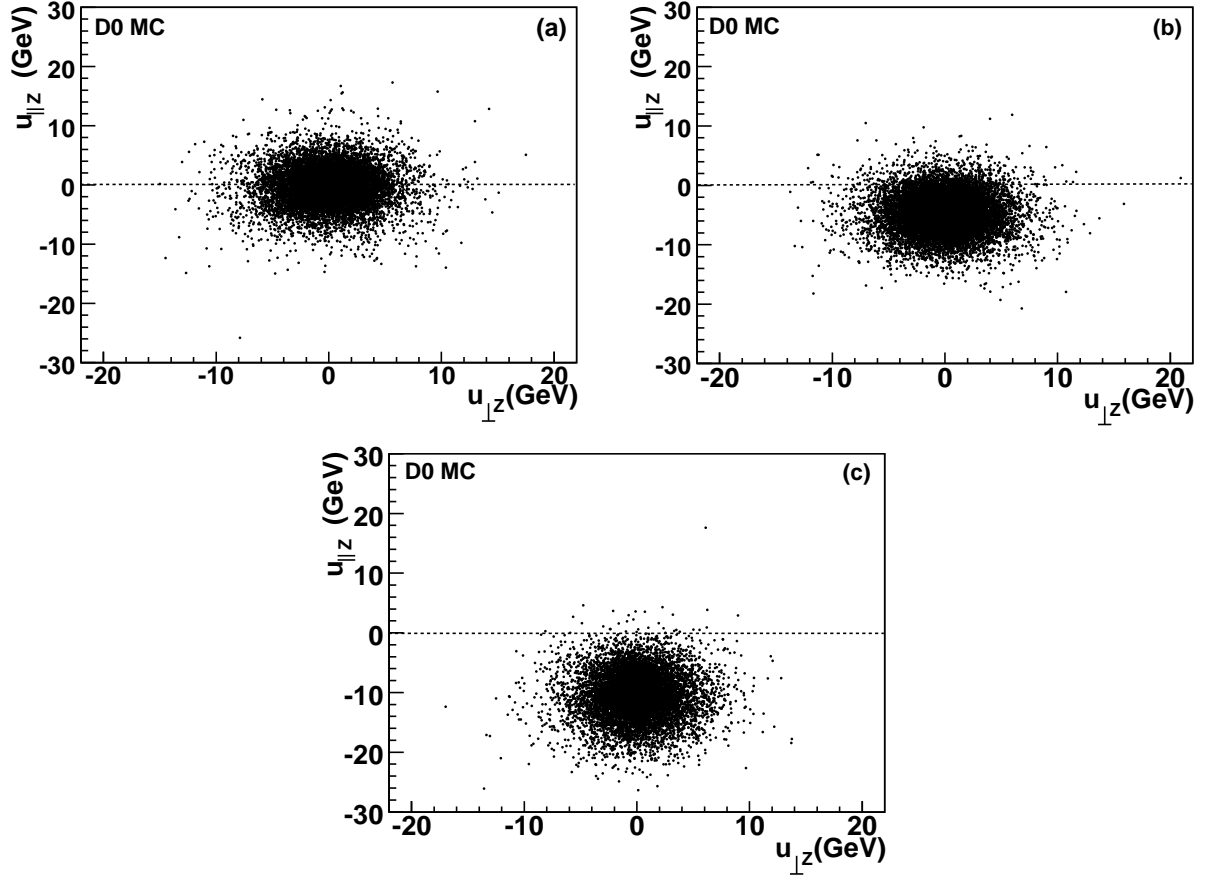
Figure 3: Examples of the distribution of the component of the measured recoil parallel ($u_{\parallel Z}$) and perpendicular ($u_{\perp Z}$) to the Z boson direction for three different bins in true $|\vec{p}_T^Z|$ (centered at (a) 0.4, (b) 10, and (c) 29 GeV). Each dot represents $\vec{u}_T$ from a single event in the library.
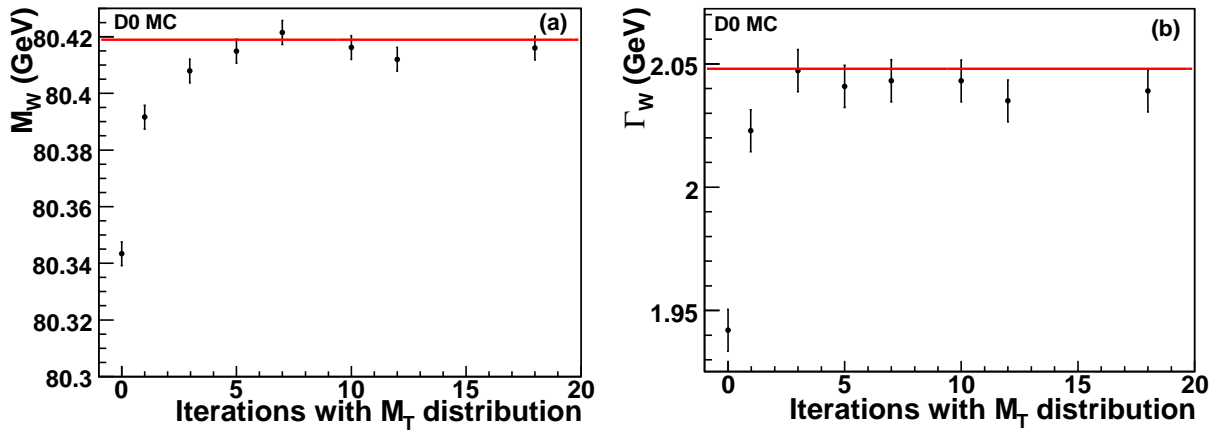
Figure 4: Estimated (a) W boson mass and (b) W boson width in fast MC using the M_T distribution, as a function of number of iterations used in the unfolding. The red line indicates the input values of W boson mass and width in the fast MC. The default number of iterations used is 10.
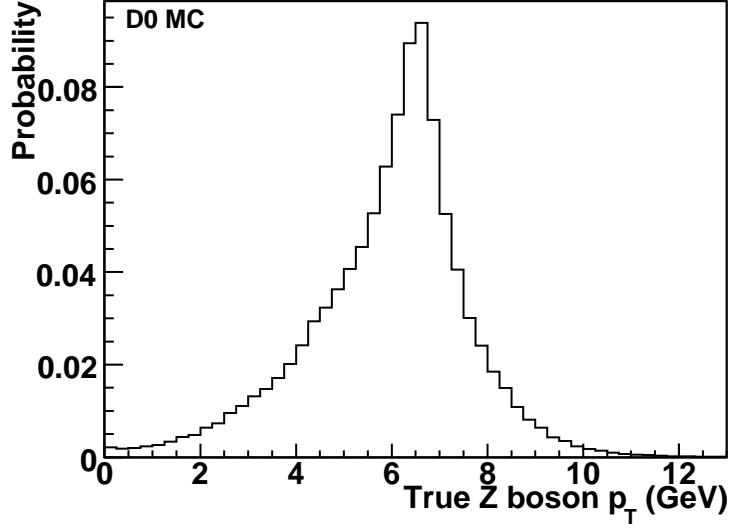
Figure 5: The distribution of the probabilities that a reconstructed $|\vec{p}_T^{\,Z}|$ of 7 GeV with corresponding $|\vec{u}_T|$ of 3.5 GeV comes from various true $|\vec{p}_T^{\,Z}|$ bins.
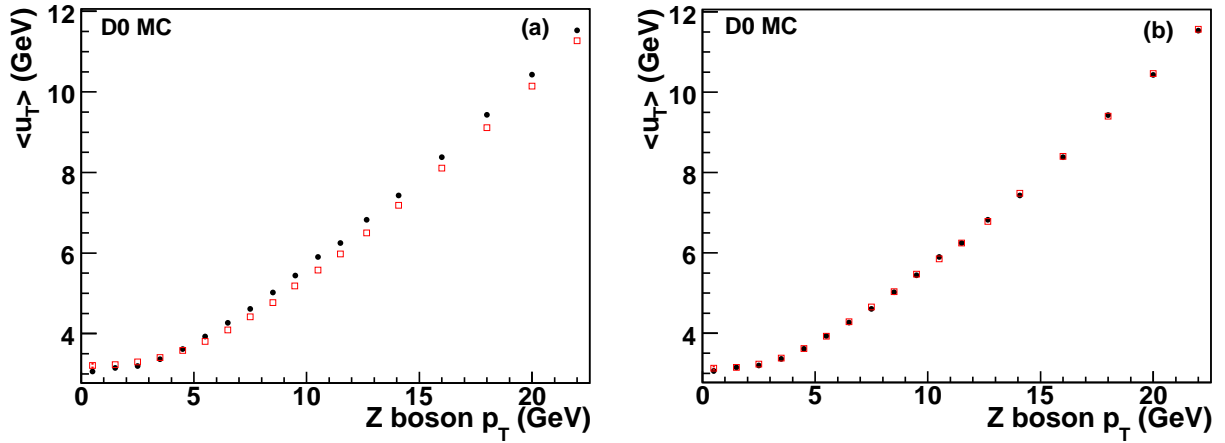

Figure 6: Mean recoil $|\vec{u}_T|$ versus true $|\vec{p}_T^{\,Z}|$ (black filled points) and mean recoil $|\vec{u}_T|$ versus the estimate of the true $\vec{p}_T^{\,Z}$ using the two electrons (red open boxes) when using (a) the two smeared electrons directly and (b) the unfolded map.
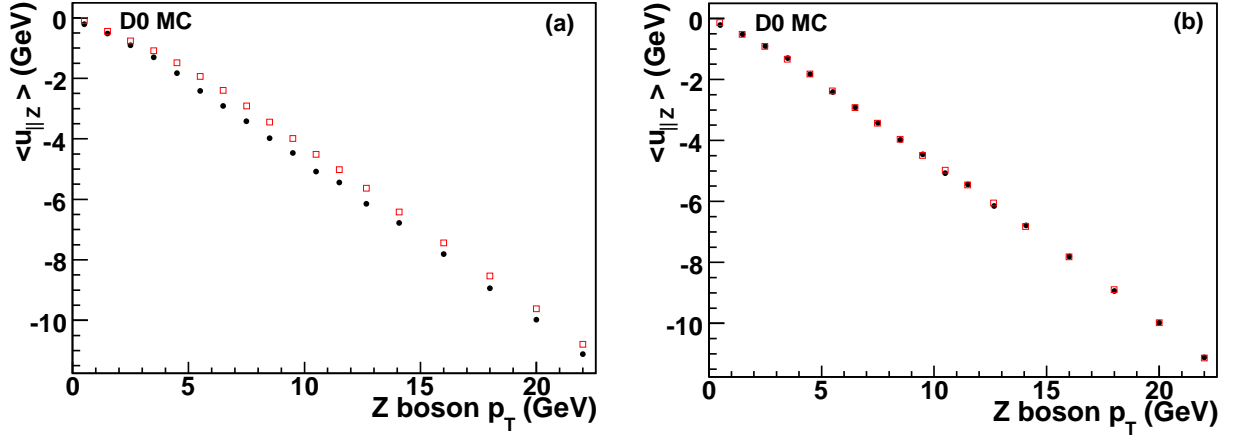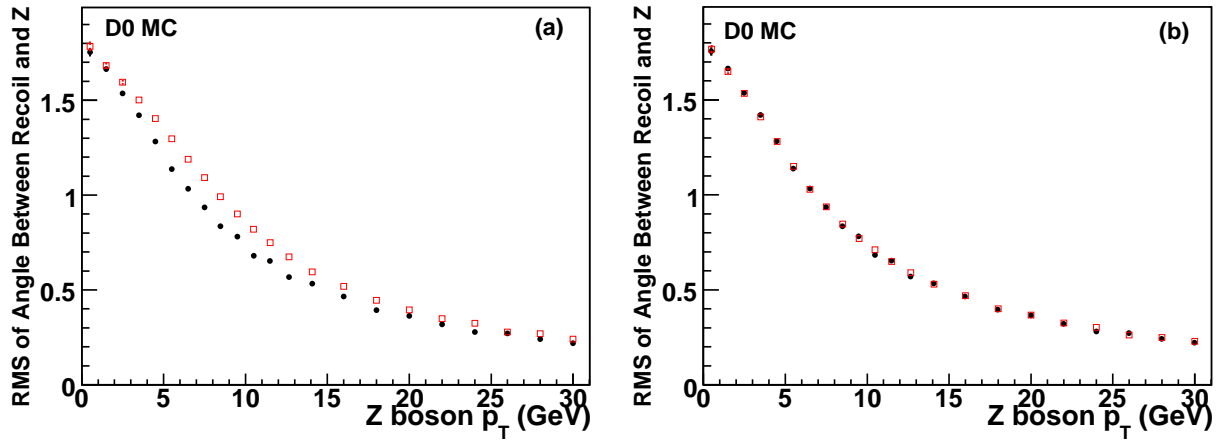
Figure 7: Mean projection of the recoil along the Z boson direction ($< u_{\parallel Z} >$) versus true $|\vec{p}_T^Z|$ (black filled points) and mean projection of the recoil along the boson direction versus the estimate of the true $\vec{p}_T^Z$ using the two electrons (red open boxes) when using (a) the two smeared electrons directly and (b) the unfolded map.

Figure 8: RMS of the opening angle between $\vec{u}_T$ and $\vec{p}_T^Z$ versus true $\vec{p}_T^Z$ (black filled points) and RMS of the opening angle between the recoil and the boson versus the estimate of the true $|\vec{p}_T^Z|$ using the two electrons (red open boxes) when using (a) the two smeared electrons directly and (b) the unfolded map.
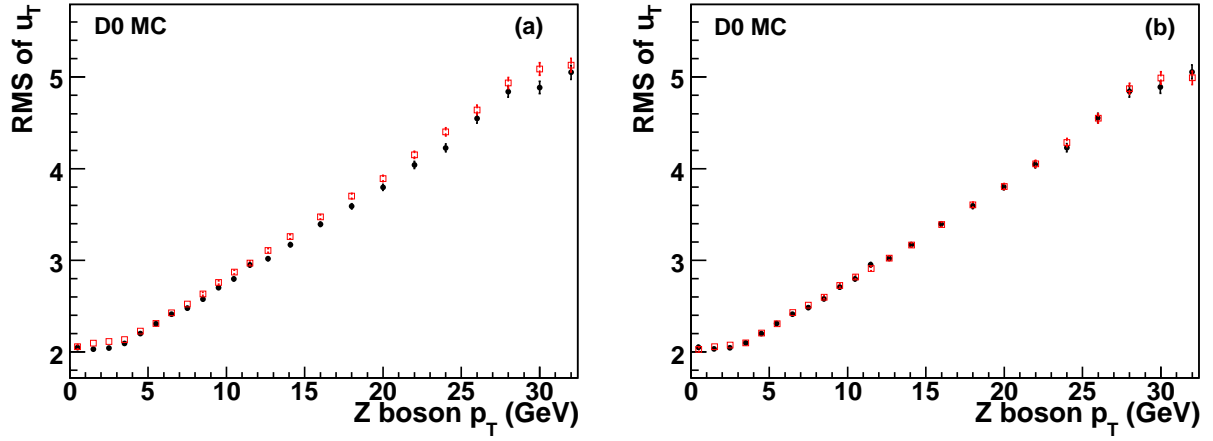
Figure 9: RMS of the recoil $|\vec{u}_T|$ versus true $|\vec{p}_T^Z|$ (black filled points) and RMS of the recoil $|\vec{u}_T|$ versus the estimate of the true $|\vec{p}_T^Z|$ using the two electrons (red open boxes) when using (a) the two smeared electrons directly and (b) the unfolded map.
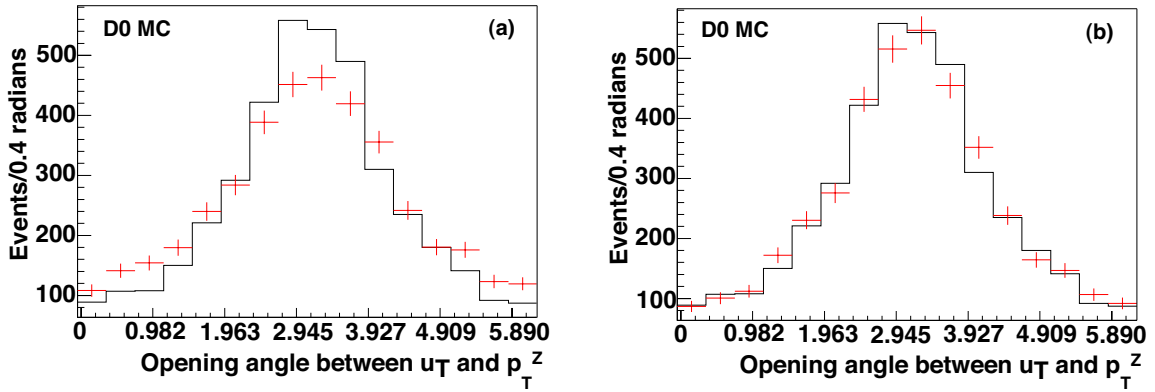

Figure 10: Opening angle between $\vec{u}_T$ and true $\vec{p}_T^Z$ (solid line) and opening angle between $\vec{u}_T$ and the estimated direction of true $\vec{p}_T^Z$ (points) when using (a) the two smeared electrons directly and (b) the unfolded map for Z boson events with a true $|\vec{p}_T^Z|$ of 4.0 to 4.25 GeV.
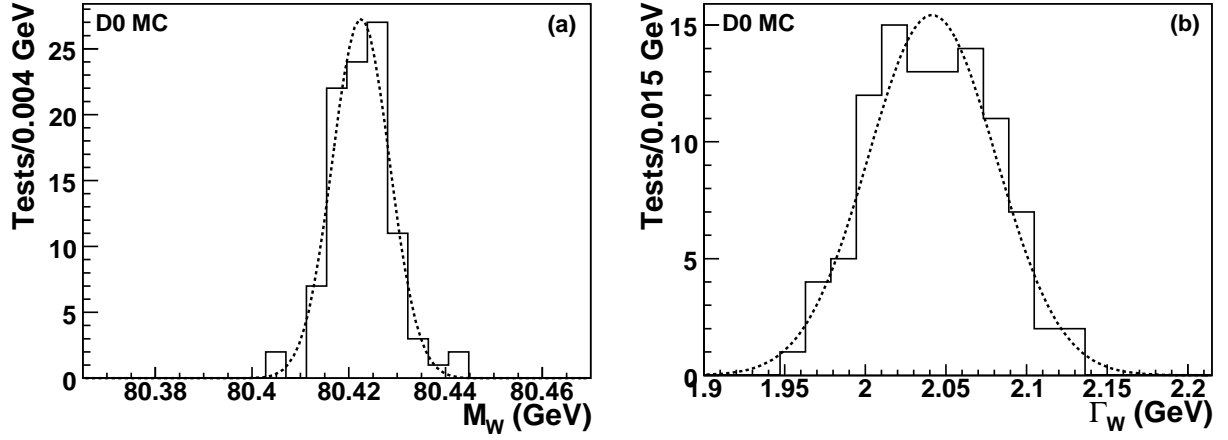
Figure 11: (a) W boson mass and (b) width measured in 100 ensemble tests for each template generated from a recoil file. The dash line is a fit using a Gaussian function. All ensembles were generated with an input W boson mass of 80.419 GeV and width of 2.039 GeV. The fitted gaussian function for the mass has a mean value of 80.420 ± 0.001 GeV and RMS of 0.005 ± 0.001 GeV. The values for the width are 2.040 ± 0.001 GeV (mean) and 0.040 ± 0.003 (RMS) GeV.
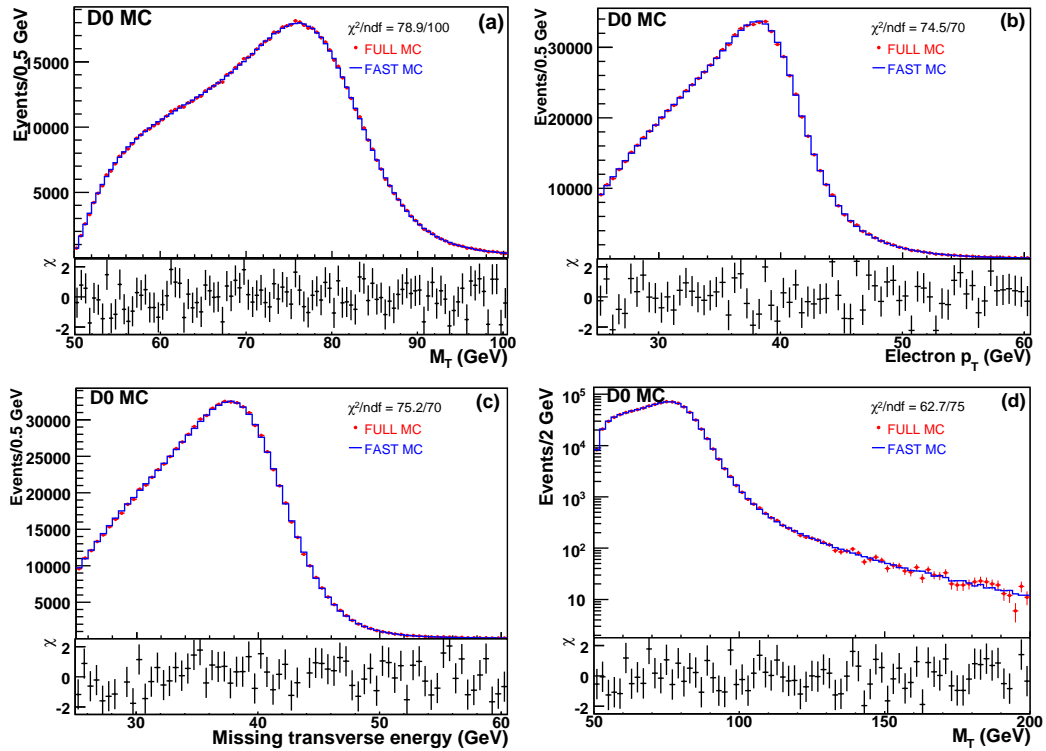

Figure 12: Comparison plots between full MC (points) and fast MC produced using the recoil library (lines) for the W boson (a) M_T, (b) $|\vec{p}_T^{\,e}|$, (c) $|\vec{\not{E}}_T|$, and (d) M_T (log scale) distributions. Also shown are the χ values defined as the difference between full MC and fast MC yields divided by the statistical uncertainty on the full MC yield. Different ranges and bin sizes are used for (a) and (d).

Table 1: Total systematic uncertainties on the W boson mass and width from the recoil library method, for 1 fb^{-1} of Z boson data.

Source	$\Delta M_W(M_T)$ (MeV)	$\Delta M_W(|\vec{p}_T^{\,e}|)$ (MeV)	$\Delta M_W(|\vec{\rlap{/}{p}}_T|)$ (MeV)	$\Delta \Gamma_W(M_T)$ (MeV)
Recoil statistics	5	8	17	40
FSR photons	1	2	2	1
Efficiency related bias	7	7	8	7
$\Delta u_\parallel^e$	2	4	1	7
Unfolding	3	3	3	3
Systematic total	9	12	19	41

Table 2: Final result of the full MC closure fits for the W boson mass and width using the recoil library method. The full MC samples used here are equivalent to 2.5 fb^{-1} of W boson data and 6.0 fb^{-1} of Z boson data. For the fitted W boson mass and width, the first uncertainty is statistical, the second is the systematic on the electron simulation, the third is the systematic on the recoil system simulation due to Z boson statistics, and the fourth is other systematics on the recoil system simulation. ΔM_W represents the difference between the measured W boson mass and the input value of 80.450 GeV, and $\Delta \Gamma_W$ represents the difference between the measured W boson width and the input value of 2.071 GeV.

Observable	ΔM_W (MeV)
M_T	$6 \pm 15 \pm 15 \pm 2 \pm 7$
$|\vec{p}_T^{\,e}|$	$5 \pm 19 \pm 12 \pm 3 \pm 8$
$|\vec{\rlap{/}{p}}_T|$	$0 \pm 19 \pm 15 \pm 7 \pm 8$
	$\Delta \Gamma_W$ (MeV)
M_T	$-5 \pm 27 \pm 15 \pm 16 \pm 10$